Reaction Mechanisms

DOI: 10.1002/anie.201103710

Insights into the Mechanism of Photocatalytic Water Reduction by DFT-Supported In Situ EPR/Raman Spectroscopy**

Dirk Hollmann, Felix Gärtner, Ralf Ludwig, Enrico Barsch, Henrik Junge, Matthias Blug, Sascha Hoch, Matthias Beller,* and Angelika Brückner**

Dedicated to the Fritz Haber Institute, Berlin, on the occasion of its 100th anniversary

Considering the foreseeable shortage of fossil resources and global warming, the development of sustainable-energy technologies is of vital interest.[1] An attractive option for the production of more benign energy vectors is the generation of hydrogen by photocatalytic water reduction. This concept facilitates the transformation of sunlight as the ultimate energy source into transportable energy carriers such as hydrogen. Hence, significant efforts are currently being undertaken to increase the activity and stability of suitable water-splitting catalysts.[2,3] The overall process can be divided into the two half reactions: water oxidation[4] and water reduction.[5] Studying these half reactions in detail, in particular the formation, operation, and decomposition of the catalyst, provides essential information for the development of new more efficient and environmentally benign catalysts. Recently, the Beller group disclosed an efficient water-reduction catalyst system consisting of $[Ir(ppy)_2(bpy)]PF_6$ (ppy = 2-phenylpyridine, bpy = 2,2′-bipyridine) as photosenzitizer (IrPS),[6] $[Fe_3(CO)_{12}]$ as water-reduction catalyst (WRC), and triethylamine (TEA) as sacrificial reductant (SR; Scheme 1).[7]

It is supposed that the catalytic cycle starts by photoexcitation of IrPS and charge separation, and subsequent reduction of its excited state by TEA (SR, cycle I). From the reduced state $IrPS^-$ an electron is transferred to the WRC, which subsequently reduces aqueous protons to H_2 (cycle II).

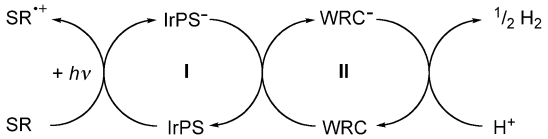

Scheme 1. General principle of H_2 formation through the photocatalytic water-reduction cascade.

To date, the only intermediate that has been experimentally identified by in situ IR spectroscopy in the water-reduction cascade (Scheme 1) is the anion $[HFe_3(CO)_{11}]^-$, which is considered to be the catalytically active species.[8] However, the preceding steps leading to its formation as well as pathways responsible for the observed deactivation with time are still not known. Thus, more comprehensive in situ studies using additional methods are highly desired. It is probable that the one-electron-transfer processes in the catalytic cycles I and II (Scheme 1) lead to paramagnetic radical intermediates. Such species are accessible by EPR spectroscopy, while the diamagnetic $[HFe_3(CO)_{11}]^-$ anion is EPR-silent but can be observed by vibrational in situ spectroscopic methods.

To gain a more detailed insight into catalytic cycles I and II and to identify possible deactivation processes, we have monitored the reaction simultaneously by in situ EPR/Raman spectroscopy. To the best of our knowledge, photocatalytic water-splitting reactions have never been studied by these coupled techniques. The interpretation of our experimental data is supported by DFT calculations and additional in situ IR studies.

First, catalytic cycle I was investigated. As expected, the IrPS complex (low-spin d^6, diamagnetic) showed no EPR signal in a solution containing THF/TEA/H_2O (8:2:1) in the absence of $[Fe_3(CO)_{12}]$ without light irradiation. However, if this solution is irradiated at 300 K, an intense isotropic signal at $g = 1.9840$ is observed (Figure 1). This signal corresponds to the reduced form of the iridium photosensitizer ($IrPS^-$), which is formed by reductive quenching of the excited state (IrPS*) by TEA.[6] A similar signal was formed neither in pure THF nor in THF/H_2O, suggesting that 1) TEA is needed as a reducing agent and 2) excitation by light is essential to initiate the electron transfer. However, it must also be mentioned that the signal rapidly declines with time, probably because of ligand dissociation from $IrPS^-$ (for additional information see Figure SI1 in the Supporting Information). In a reaction mixture containing all the necessary components of the water-reduction system (THF, H_2O, TEA, IrPS, and Fe-WRC), no

[*] Dr. D. Hollmann, F. Gärtner, Prof. Dr. R. Ludwig, E. Barsch, Dr. H. Junge, Prof. Dr. M. Beller, Prof. Dr. A. Brückner
Leibniz-Institut für Katalyse an der Universität Rostock e.V.
Albert-Einstein-Strasse 29a, 18059 Rostock (Germany)
E-mail: matthias.beller@catalysis.de
angelika.brueckner@catalysis.de
Homepage: http://www.catalysis.de
Prof. Dr. R. Ludwig, E. Barsch
Universität Rostock, Institut für Chemie
Abteilung Physikalische Chemie
Dr. Lorenz Weg 1, 18059 Rostock (Germany)
E-mail: ralf.ludwig@uni-rostock.de
Dr. M. Blug, Dr. S. Hoch
Evonik Degussa GmbH, Creavis Technologies & Innovation
Paul-Baumann-Strasse 1, 45772 Marl (Germany)

[**] This work was supported by Evonik Degussa GmbH (financed in part by the State of North Rhine Westphalia and cofinanced by the European Union Investing in our Future, European Regional Development Fund). F.G. thanks the Fonds der Chemischen Industrie for a Kekulé grant. DFT = density functional theory.

Supporting information for this article is available on the WWW under http://dx.doi.org/10.1002/anie.201103710.

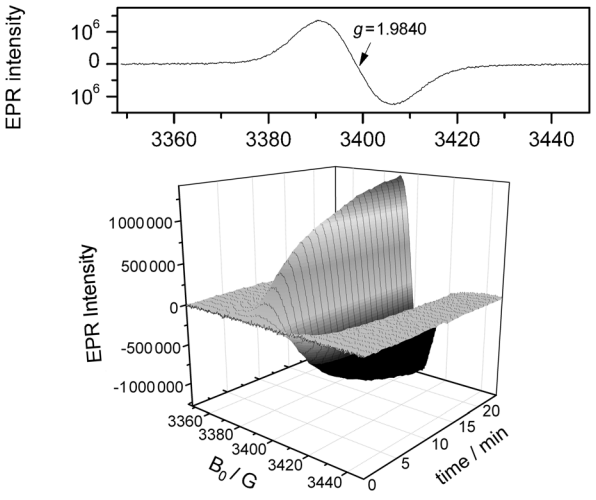

Figure 1. EPR spectra of $[Ir(ppy)_2(bpy)]PF_6$ (**1**) in THF/TEA/H_2O (8:2:1) under irradiation at 300 K. Top: signal after 20 min, bottom: time-dependent plot.

$IrPS^-$ signal is observed during irradiation. This can be explained by a fast intermolecular electron transfer to the Fe-WRC (Figure SI2 in the Supporting Information), which limits the lifetime of the transient paramagnetic $IrPS^-$ species.

Surprisingly, during our EPR studies we detected a new unexpected TEA radical (Figure SI3 in the Supporting Information). According to the anticipated reaction mechanism, one-electron transfer from TEA to the IrPS should convert the sacrificial reagent to a $N^{\bullet+}(CH_2CH_3)_3$ species in which the unpaired electron is located at the N atom. Hence, hyperfine splitting (hfs) due to coupling of the electron with the nuclear spin of ^{14}N (I = 1) and six ^1H (I = 1/2) from the three α-CH_2 groups is expected.[9–11] However, it was also found that the half-life of the analogous $Pr_3N^{\bullet+}$ species is only $\tau_{1/2} \approx 0.2$ ms at 300 K.[9] Unexpectedly, in our experiments we could not detect a similar $TEA^{\bullet+}$ EPR signal consistent with the above-mentioned hfs pattern. Instead we found a multiplet characteristic of a $R_2NCH_2C^{\bullet}H_2$ radical (R = Et or H) which shows hfs from the single electron on the β-C atom with two sets of two equivalent protons on the α- and β-C atoms. For reasons which are discussed in more detail in the Supporting Information (Figures SI3 and SI5, Scheme SI4), we assign this signal to the primary $H_2NCH_2C^{\bullet}H_2$ radical or the $H_2N^+CH_2C^{\bullet}H_2$ radical cation which is formed as a result of oxidative degradation of TEA.

After investigation of the IrPS cycle I we were interested in the Fe-WRC cycle II. Since $[Fe_3(CO)_{12}]$ can form both dia- and paramagnetic species, coupled in situ EPR/Raman spectroscopy, combined with in situ IR spectroscopy, is an ideal tool for the evaluation of this catalytic cycle. The relevant EPR signals and Raman and IR vibrations are displayed in Figure 2. The optimal temperature for EPR measurements was found to be 200 K (see Figure SI6 in the Supporting Information). In the Raman spectra, the metal–metal vibrations (below 300 cm^{-1}) are used to identify the iron species. Based on DFT calculations (see SI-D in the Supporting Information), these bands were assigned to Fe–Fe vibrations in the trinuclear iron cluster $[HFe_3(CO)_{11}]^-$.

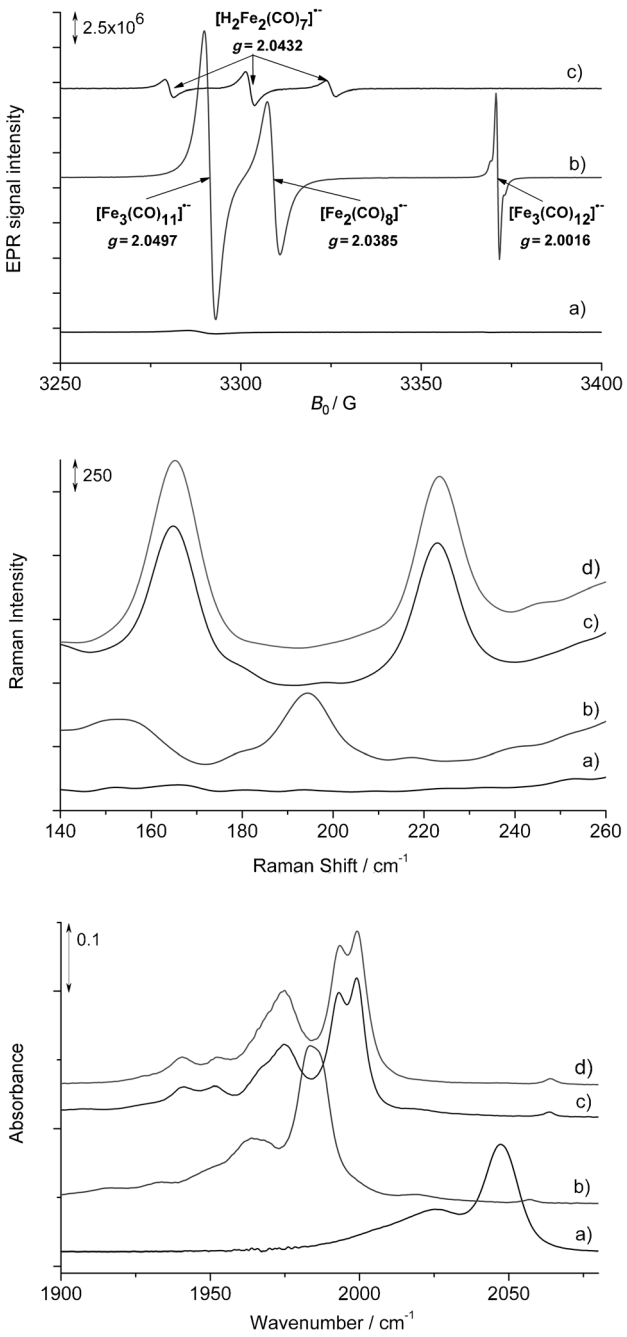

Figure 2. EPR signals of Fe radicals (top), Raman bands of Fe–Fe vibrations (middle), and FTIR bands of terminal Fe–CO vibrations (bottom) during the iron-catalyzed reduction of water: a) $[Fe_3(CO)_{12}]$ in THF; b) $[Fe_3(CO)_{12}]$ and IrPS in THF/TEA/H_2O (8:2:1) without irradiation; c) $[Fe_3(CO)_{12}]$ and IrPS in THF/TEA/H_2O (8:2:1) after 2 min irradiation; d) $[HFe_3(CO)_{11}]^-$ in THF.

First, $[Fe_3(CO)_{12}]$ was investigated in THF without irradiation (Figure 2a). Neither an EPR signal nor Raman bands were observed. The IR spectrum of $[Fe_3(CO)_{12}]$ shows two bands at 2047 and 2025 cm^{-1} arising from the terminal CO vibration.[12] In contrast, a solution of IrPS and Fe-WRC in THF/TEA/H_2O (8:2:1) in the absence of irradiation shows already three narrow EPR signals (Figure 2b). Based on their *g* values, they can be assigned to the radicals $[Fe_3(CO)_{12}]^{\bullet-}$

($g = 2.0016$), $[Fe_3(CO)_{11}]^{\bullet-}$ ($g = 2.0497$), and $[Fe_2(CO)_8]^{\bullet-}$ ($g = 2.0385$).[13,14] The total initial spin concentration corresponds to 94% of the overall Fe content in the solution and the ratio of the three radicals amounts to 1:66:32.

The corresponding Raman spectrum shows a band at 194 cm^{-1} (Figure 2b), which is attributed to the Fe–Fe vibration of the binuclear radical anion $[Fe_2(CO)_8]^{-\bullet}$. This band is in good agreement with the Fe–Fe Raman vibration of the dinuclear $[dmted]^{2+}[Fe_2(CO)_8]^{2-}$ (dmted = *N*,*N*′-dimethyltriethylenediamine) cluster at 178 cm^{-1} observed by Onaka and Shriver.[15]

Under irradiation (Figure 2c), all three EPR radicals disappear and a new triplet at $g = 2.0433$ arises, which was assigned to $[H_2Fe_2(CO)_7]^{\bullet-}$ and is discussed in further detail below. A typical time-dependent EPR plot is displayed in Figure SI7 in the Supporting Information. However, the intensity of this signal reflects only 3% of the total iron content in solution. This suggests that the dominating iron-containing species under the reaction conditions is EPR-silent. Raman and IR spectra (Figure 2c) suggest that the major Fe component is the diamagnetic $[HFe_3(CO)_{11}]^-$ anion, which was also found by in situ IR measurements.[8] In the corresponding Raman spectrum (after 2 min), two new bands appear at 223 and 165 cm^{-1} which are attributed to the Fe–Fe vibrations 1 and 2 denoted in Figure 3. To the best of our knowledge, no Fe–Fe Raman vibrations of trinuclear iron clusters in solution have been reported so far.[16] Thus, we performed DFT calculations of the $[HFe_3(CO)_{11}]^-$ anion. The calculated Raman frequencies (172 and 230 cm^{-1}) are in good agreement with experimental frequencies. In the IR spectrum new bands arise at 1999, 1993, and 1975 cm^{-1} (Figure 2c). The reliable assignment of the IR and Raman bands is confirmed by the fact that a separately prepared $[HNEt_3]^+[HFe_3(CO)_{11}]^-$ complex[17] in THF solution shows identical FTIR and Raman spectra (Figure 2d).

After prolonged irradiation (> 2 min), the EPR and Raman spectra did not change further. This is in agreement with the results of previous in situ IR measurements,[8] which identified $[HFe_3(CO)_{11}]^-$ as the active species for hydrogen production.

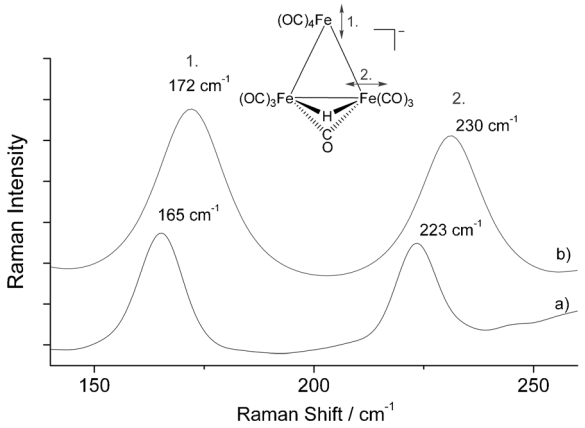

Figure 3. a) Experimental and b) DFT-calculated Fe–Fe Raman vibrations of $[HFe_3(CO)_{11}]^-$.

Based on the results obtained by the three spectroscopic methods along with DFT calculations, a detailed mechanism for the formation of the active $[HFe_3(CO)_{11}]^-$ complex and its role in hydrogen evolution can be proposed (Scheme 2). Notably, these studies also shed light on the experimentally observed but still poorly understood deactivation of the iron catalyst at extended irradiation times: Initially, the diamagnetic $[Fe_3(CO)_{12}]$ complex is quickly reduced by electron transfer, forming the formal electron-rich 19e complex $[Fe_3(CO)_{12}]^{\bullet-}$ which is not stable and decomposes into the electron-deficient 17e complex $[Fe_3(CO)_{11}]^{\bullet-}$ by decarbonylation as well as into $[Fe_2(CO)_8]^{\bullet-}$ and a tentative diamagnetic $[Fe(CO)_4X]$ species by incorporation of CO or a solvent molecule.

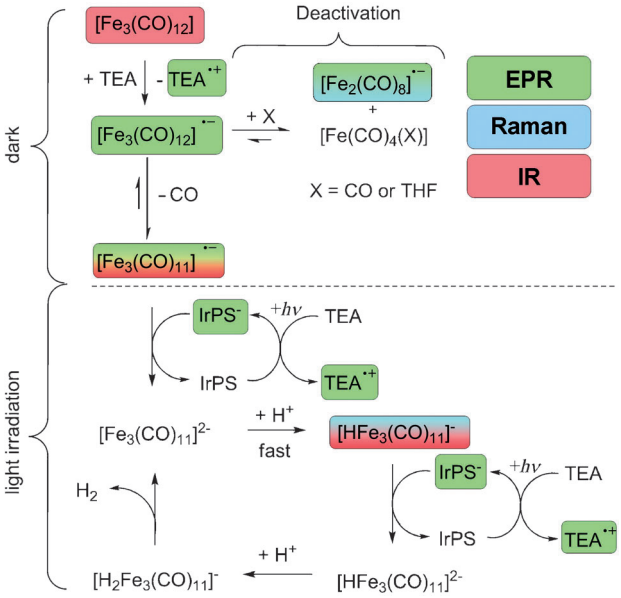

Scheme 2. Proposed reaction mechanism (spectroscopically detected intermediates are highlighted).

Notably, these reactions occur already in the dark. Under light irradiation, $[Fe_3(CO)_{11}]^{\bullet-}$ is converted by electron transfer from the $IrPS^-$ and subsequent proton transfer to the active $[HFe_3(CO)_{11}]^-$ catalyst. A second electron/proton transfer is supposed to form H_2 via a transient dihydrido ironcarbonyl species that restores the $[Fe_3(CO)_{11}]^{2-}$ anion which starts the cycle again.

During testing, a gradual decline of the catalyst activity was observed, which was accompanied by CO evolution (up to 0.5 vol%).[8] Taking into account the detection of $[H_2Fe_2(CO)_7]^{\bullet-}$ ($g = 2.0433$, $A(H) = 22.3$ G, $\Delta B = 2.36$ G)[18] and $[Fe_2(CO)_8]^{\bullet-}$ with and without light by EPR (Figure 4), deactivation through decomposition of the WRC by dinuclear iron species can be anticipated.

When a 420 nm cutoff filter was used which eliminates UV light, $[Fe_2(CO)_8]^{\bullet-}$ and $[H_2Fe_2(CO)_7]^{\bullet-}$ were hardly detected upon extended time (Scheme SI8 in the Supporting Information), yet production of hydrogen was still observed under the same conditions in catalytic tests.[7] Thus, it can be excluded that the dinuclear iron complexes are responsible

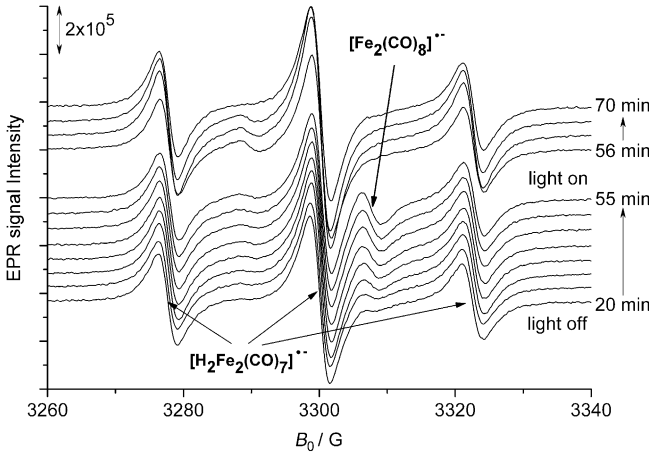

Figure 4. EPR spectra of IrPS and $[Fe_3(CO)_{12}]$ in THF/TEA/H_2O solution measured at 200 K as a function of irradiation time.

for catalytic activity. The absence of $[H_2Fe_2(CO)_7]^{\bullet-}$ and the suppressed deactivation during exclusion of UV light fits well with the prolonged stability under these conditions.[7]

In summary, we have presented a detailed investigation of the mechanism of the iridium- and iron-catalyzed water reduction. In cycle I, we studied the electron transfer from the sacrificial reductant (TEA) to the IrPS together with a novel degradation pathway of the TEA molecule. In cycle II, especially the coupling of Raman and EPR spectroscopy proved to be crucial for identifying paramagnetic iron clusters starting from $[Fe_3(CO)_{12}]$ and their conversion to the active catalyst species $[HFe_3(CO)_{11}]^-$, whereby the assignment of new Fe–Fe Raman bands was substantially supported by DFT results. Based on our mechanistic studies, the development of improved water-reduction catalysts should be possible in a more rational manner. Finally, such information will also be the basis for optimizing the combination of the two half cycles in the overall water-splitting process.

Experimental Section

In situ EPR spectra in X-band were recorded by a Bruker EMX CW-microspectrometer using an ER 4119HS-WI high-sensitivity optical resonator with a grid on the front side. The temperature was adjusted by a Bruker Digital Temperature Control System ER4131VT. For EPR/Raman measurements under light irradiation, the beam of a Lot-Oriel 300 W Xe lamp (LSB530) with a UV cutoff filter (GG420) and the 532 nm laser beam of a RXN Raman spectrometer (Kaiser Optical Systems) were focused on the sample by optical fibers. To avoid disturbance of the Raman measurements by UV/Vis irradiation, Raman spectra were recorded before and after excitation. For these measurements, 50 μL of a freshly prepared stock solution of $[Ir(ppy)_2(bpy)]PF_6$ (0.60 mg, 0.75 μmol) and $[Fe_3(CO)_{12}]$ (0.93 mg, 1.85 μmol) in THF/TEA/H_2O (8:2:1; 1 mL) was filled in a 3 mm EPR tube under argon. The g values were calculated from the resonance field B_0 and the resonance frequency ν using the resonance condition $h\nu = g\beta B_0$. The standard deviation is ± 0.00004. The spin concentration was determined by comparing the signal intensities (double integrals) with that of a solution of the TEMPO[19] radical in THF/TEA/H_2O (8:2:1). The EPR spectra were simulated using the program Sim14S[20] (IrPS) and the Bruker Simfonia program (TEA). FTIR measurements were carried out on a Bruker Matrix spectrometer equipped with an MCT detector. The optics were purged with dry air. The reaction was carried out under inert gas atmosphere. A micro gear pump was used to circulate the reaction solution continuously through a demountable IR cell. The window material was ZnS. To avoid fringes in the examined spectral range, a wedged spacer with a mean optical path length of 0.48 mm was used. Geometry optimizations of $[HFe_3(CO)_{11}]^-$ were carried out using the Gaussian 03 program package[21] with the B3PW91 gradient corrected hybrid density functional[22] (B3PW91/6-31G*) to calculate the structure and vibrational frequencies. No imaginary frequencies were found, indicating that at least local minimum structures were identified on the potential energy surface. In agreement with the average scaling factor of 0.96 given for this level of theory, the calculated frequencies are about 4% larger than the measured frequencies.[23]

Received: May 31, 2011
Published online: August 10, 2011

Keywords: density functional calculations · EPR spectroscopy · iron · Raman spectroscopy · photocatalytic water splitting

[1] a) Q. Schiermeier, J. Tollefson, T. Scully, A. Witze, O. Morton, *Nature* **2008**, *454*, 816; b) N. Armaroli, V. Balzani, *Angew. Chem.* **2007**, *119*, 52; *Angew. Chem. Int. Ed.* **2007**, *46*, 52.

[2] For recent reviews on water-splitting catalysts, see: a) M. Kitano, M. Hara, *J. Mater. Chem.* **2010**, *20*, 627; b) A. Kudo, Y. Miseki, *Chem. Soc. Rev.* **2009**, *38*, 253; c) L. L. Tinker, N. D. McDaniel, S. Bernhard, *J. Mater. Chem.* **2009**, *19*, 3328; d) Y. Inoue, *Energy Environ. Sci.* **2009**, *2*, 364; e) F. E. Osterloh, *Chem. Mater.* **2008**, *20*, 35.

[3] Selected examples of recent publications on water-splitting catalysts: a) J. Zhang, J. Sun, K. Maeda, K. Domen, P. Liu, M. Antonietti, X. Fu, X. Wang, *Energy Environ. Sci.* **2011**, *4*, 675; b) K. Maeda, A. Xiong, T. Yoshinaga, T. Ikeda, N. Sakamoto, T. Hisatomi, M. Takashima, D. Lu, M. Kanehara, T. Setoyama, T. Teranishi, K. Domen, *Angew. Chem.* **2010**, *122*, 4190; *Angew. Chem. Int. Ed.* **2010**, *49*, 4096; c) K. Maeda, M. Higashi, D. Lu, R. Abe, K. Domen, *J. Am. Chem. Soc.* **2010**, *132*, 5858.

[4] Selected recent publications on homogeneous water-oxidation catalysts: a) G. Armstrong, *Nat. Chem.* **2010**, DOI: 10.1038/nchem.958; b) Z. Chen, J. J. Concepcion, H. Luo, J. F. Hull, A. Paul, T. J. Meyer, *J. Am. Chem. Soc.* **2010**, *132*, 17670; c) W. C. Ellis, N. D. McDaniel, S. Bernhard, T. J. Collins, *J. Am. Chem. Soc.* **2010**, *132*, 10990; d) D. J. Wasylenko, C. Ganesamoorthy, B. D. Koivisto, M. A. Henderson, C. P. Berlinguette, *Inorg. Chem.* **2010**, *49*, 2202; e) J. J. Concepcion, J. W. Jurss, M. R. Norris, Z. Chen, J. L. Templeton, T. J. Meyer, *Inorg. Chem.* **2010**, *49*, 1277; f) L. Duan, Y. Xu, P. Zhang, M. Wang, L. Sun, *Inorg. Chem.* **2010**, *49*, 209; g) J. F. Hull, D. Balcells, J. D. Blakemore, C. D. Incarvito, O. Eisenstein, G. W. Brudvig, R. H. Crabtree, *J. Am. Chem. Soc.* **2009**, *131*, 8730.

[5] Selected recent publications on homogeneous water- reduction catalysts: a) F. Gärtner, D. Cozzula, S. Losse, A. Boddien, G. Anilkumar, H. Junge, T. Schulz, N. Marquet, A. Spannenberg, S. Gladiali, M. Beller, *Chem. Eur. J.* **2011**, *17*, 6998; b) J. D. Knoll, S. M. Arachchige, K. J. Brewer, *ChemSusChem* **2011**, *4*, 252; c) T. M. McCormick, B. D. Calitree, A. Orchard, N. D. Kraut, F. V. Bright, M. R. Detty, R. Eisenberg, *J. Am. Chem. Soc.* **2010**, *132*, 15480; d) P. Zhang, M. Wang, Y. Na, X. Li, Y. Jiang, L. Sun, *Dalton Trans.* **2010**, *39*, 1204; e) D. Streich, Y. Astuti, M. Orlandi, L. Schwartz, R. Lomoth, L. Hammarström, S. Ott, *Chem. Eur. J.* **2010**, *16*, 60; f) B. Probst, A. Rodenberg, M. Guttentag, P. Hamm, R. Alberto, *Inorg. Chem.* **2010**, *49*, 6453; g) M. Wang, Y. Na, M. Gorlov, L. Sun, *Dalton Trans.* **2009**, 6458.

[6] The quenching process for this and analogous iridium complexes have been studied mainly by luminescence and UV/Vis spectroscopy: a) L. L. Tinker, S. Bernhard, *Inorg. Chem.* **2009**, *48*, 10507; b) P. N. Curtin, L. L. Tinker, C. M. Burgess, E. D. Cline, S. Bernhard, *Inorg. Chem.* **2009**, *48*, 10498; c) E. D. Cline, S. E. Adamson, S. Bernhard, *Inorg. Chem.* **2008**, *47*, 10378; d) L. L. Tinker, N. D. McDaniel, P. N. Curtin, C. K. Smith, M. J. Ireland, S. Bernhard, *Chem. Eur. J.* **2007**, *13*, 8726; e) J. I. Goldsmith, W. R. Hudson, M. S. Lowry, T. H. Anderson, S. Bernhard, *J. Am. Chem. Soc.* **2005**, *127*, 7502.

[7] F. Gärtner, B. Sundararaju, A.-E. Surkus, A. Boddien, B. Loges, H. Junge, P. H. Dixneuf, M. Beller, *Angew. Chem.* **2009**, *121*, 10147; *Angew. Chem. Int. Ed.* **2009**, *48*, 9962.

[8] F. Gärtner, A. Boddien, E. Barsch, K. Fumino, S. Losse, H. Junge, D. Hollmann, A. Brückner, R. Ludwig, M. Beller, *Chem. Eur. J.* **2011**, *17*, 6425.

[9] CW EPR spectra of $Pr_3N^{\bullet+}$: W. Miao, J.-P. Choi, A. J. Bard, *J. Am. Chem. Soc.* **2002**, *124*, 14478.

[10] CW EPR spectra of $Et_3N^{\bullet+}$in $AlPO_4$: W. Liu, S. Yamanaka, M. Shiotani, J. Michalik, A. Lund, *Phys. Chem. Chem. Phys.* **2001**, *3*, 1611.

[11] FT EPR spectra of $Et_3N^{\bullet+}$: a) J.-M. Lu, D. Beckert, *Res. Chem. Intermed.* **2000**, *26*, 621; b) J. Säuberlich, O. Brede, D. Beckert, *J. Phys. Chem. A* **1997**, *101*, 5659.

[12] S. Dobos, S. Nunziante-Cesaro, M. Maltese, *Inorg. Chim. Acta* **1986**, *113*, 167.

[13] Review: Y. A. Belousov, *Russ. Chem. Rev.* **2007**, *76*, 41.

[14] Excellent assignment of the radicals through the use of ^{57}Fe and ^{18}CO labels was described by Krusic et al.: a) P. J. Krusic, J. S. Filippo, Jr., B. B. Hutchinson, R. L. Hance, L. M. Daniels, *J. Am. Chem. Soc.* **1981**, *103*, 2129; b) P. J. Krusic, *J. Am. Chem. Soc.* **1981**, *103*, 2131.

[15] S. Onaka, D. F. Shriver, *Inorg. Chem.* **1976**, *15*, 915.

[16] At room temperature no Raman signal for the trinuclear iron complexes $[Fe_3(CO)_{12}]$ and $[Fe_3(CO)_{11}]^{\bullet-}$ are observed. Shriver et al. were able to measure the Raman spectra of $[Fe_3(CO)_{12}]$ only at 10 K: C. B. Cooper III, S. Onaka, D. F. Shriver, L. Daniels. R. L. Hance, B. Hutchinson, R. Shipley, *Inorg. Chim. Acta* **1977**, *24*, L92.

[17] W. McFarlane, G. Wilkinson, W. Hübel, *Inorg. Synth.* **1966**, *8*, 181.

[18] Y. A. Belousov, *Russ. Chem. Bull.* **1997**, *46*, 1010.

[19] TEMPO = 2,2,6,6-Tetramethylpiperidine-1-oxyl.

[20] Sim14S program: G. P. Lozos, B. M. Hoffman, C. G. Franz, Quantum Chemistry, Programs Exchange **1973**, no. 265.

[21] Gaussian 03 (Revision D.01), M. J. Frisch, et al. Gaussian Inc., Wallingford, CT, **2004**, see the Supporting Information.

[22] a) A. B. Becke, *J. Chem. Phys.* **1993**, *98*, 5648; b) J. P. Perdew, Y. Wang, *Phys. Rev. B* **1992**, *45*, 13244.

[23] J. P. Merrick, D. Moran, L. Radom, *J. Phys. Chem. A* **2007**, *111*, 11683.

